ARTICLE NO. 79-0664R

J80-091

00023
20001

Comparison of Measured and Predicted Impedance at Grazing Incidence

Harold C. Lester* and Tony L. Parrott*
NASA Langley Research Center, Hampton, Va.

The acoustic performance of a nominal locally reacting liner specimen mounted in a grazing incidence impedance tube is analyzed. Measured standing wave ratios and null positions are compared with those predicted by a finite-element algorithm. Differences between measured and calculated wave structures may be due to extended reaction effects.

Nomenclature

c_0	= speed of sound, cm/s
f	= frequency, Hz
h	= tube width, cm
j	$=\sqrt{-1}$
k	= wavenumber, $2\pi f/c_0$
L	= tube length, cm
p	= acoustic pressure, nondimensional
SWR	= standing wave ratio, dB
u,w	= acoustic particle velocities in x, z direction, nondimensional
x,z	= rectangular coordinates, nondimensional
ZNULL	= null position, cm
ζ	= impedance, $\zeta=\theta+j\chi$, nondimensional
θ	= resistance, nondimensional
λ	= wavelength, cm
ρ_0	= density, g/cm^3
χ	= reactance, nondimensional
ω	$=2\pi f$

Subscripts

A	= axial (z) direction
G	= grazing incidence
N	= normal incidence
T	= termination

Introduction

THE literature suggests that normal incidence impedance is sufficient to predict the attenuation of sound in a duct lined with a locally reacting material.[1,2] However, since acoustic particle velocity cannot as yet be accurately measured in a direct manner, acoustic impedance must be inferred from pressure measurements using an appropriate math model. One of the simplest techniques is the standing wave tube method.[1,3] In this case, the directly measured quantities are the standing wave ratio (SWR) and (first) null position; whereas the test specimen's impedance is a boundary condition on the one-dimensional wave equation.

In this paper comparisons between measured and predicted wave structures are made for a two-degree-of-freedom liner specimen constructed with perforated face plates and honeycomb partitioned cavities. The normal impedance of the liner is determined by the standing wave method at 20 Hz intervals from 0.3 to 1.2 kHz and these data are used to predict the results of grazing incidence tests conducted over the same frequency range.

Presented as Paper 79-0664 at the AIAA 5th Aeroacoustics Conference, Seattle, Wash., March 12-14, 1979; submitted April 6, 1979; revision received Oct. 9, 1979.

Index categories: Aeroacoustics; Noise.

*Aerospace Research Engineer.

Experimental Setup and Measurement Procedures

The normal and grazing incidence specimens used in the tests are shown in Fig. 1. The liner specimens were cut from a parent material fabricated with two different depths of hexagonal aluminum honeycomb (0.953-cm cell diameter) and two perforated aluminum face plates (0.07938-cm thickness). Perforated hole diameter and separation are 0.084 and 0.0282 cm (staggered rows), respectively.

Normal Incidence Impedance Measurement

The normal incidence tests were conducted using an impedance tube having a circular cross section of 5.72-cm diameter. A 60 W acoustic driver generated a discrete frequency plane wave with sound pressure levels of about 100 dB at the test specimen surface. This pressure was measured by a 0.635-cm-diam flush-mounted microphone. The standing wave structure was probed by a 0.318-cm-diam steel probe 121.9 cm in length and supported in the center of the tube. The probe was coupled to a 1.27-cm-diam microphone by means of flexible tubing and was rigidly attached to a carriage whose position could be measured. Outputs of the microphones were amplified and conditioned by a 10-Hz constant bandwidth tracking filter. The tracking filter center frequency was controlled by a signal source oscillator. This arrangement permitted SWRs to be measured to within ± 0.1 dB and null positions (ZNULL) to within ± 0.01 cm.[4]

Table 1 presents measured normal incidence impedance data for the liner test specimen. These data were reduced by

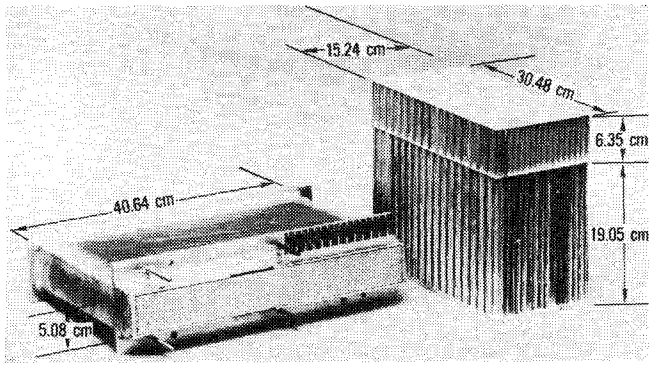

Fig. 1 Liner test specimens—normal incidence (right) and grazing incidence (left).

Table 1 Normal incidence data

Frequency, kHz	SWR, dB	ZNULL, cm	Resistance, θ_N	Reactance, x_N
0.30	14.4	54.58	0.195	-0.149
0.32	15.5	49.32	0.180	-0.260
0.34	16.2	44.53	0.178	-0.384
0.36	15.3	40.80	0.213	-0.479
0.38	17.0	37.36	0.193	-0.598
0.40	17.7	34.32	0.200	-0.720
0.42	18.0	31.60	0.220	-0.853
0.44	18.3	29.19	0.246	-0.995
0.46	18.8	27.03	0.273	-1.155
0.48	19.3	25.08	0.309	-1.337
0.50	19.4	23.28	0.377	-1.554
0.52	19.9	21.64	0.453	-1.822
0.54	20.4	20.08	0.579	-2.187
0.56	20.6	18.66	0.802	-2.650
0.58	21.1	17.30	1.201	-3.361
0.60	21.0	16.04	2.143	-4.317
0.62	20.9	14.76	5.062	-5.475
0.64	20.6	13.62	10.262	-2.148
0.66	20.2	12.47	6.849	4.780
0.68	19.5	11.31	2.737	4.200
0.70	18.6	10.20	1.416	3.036
0.72	17.0	9.06	0.910	2.178
0.74	14.7	7.94	0.722	1.592
0.76	12.9	7.08	0.658	1.274
0.78	11.7	6.29	0.602	1.053
0.80	11.2	5.49	0.526	0.883
0.82	11.0	4.68	0.456	0.734
0.84	10.6	3.63	0.396	0.549
0.86	10.7	3.07	0.363	0.467
0.88	10.8	2.23	0.325	0.339
0.90	11.1	1.66	0.299	0.256
0.92	12.1	19.31	0.251	0.094
0.94	13.1	18.09	0.222	-0.037
0.96	13.5	16.97	0.217	-0.163
0.98	13.8	15.94	0.222	-0.236
1.00	14.1	14.94	0.234	-0.421
1.02	14.0	14.06	0.263	-0.549
1.04	14.1		0.288	-0.659
1.06	14.6	12.64	0.309	-0.789
1.08	15.1	11.93	0.344	-0.949
1.10	15.5	11.20	0.410	-1.158
1.12	15.8	10.52	0.510	-1.403
1.14	15.4	9.81	0.745	-1.720
1.16	14.2	9.18	1.180	-1.972
1.18	14.8	8.48	1.923	-2.494
1.20	13.5	7.80	3.381	-2.069

the equations given in Ref. 4 using the tabulated SWR and null position ZNULL values. The impedance components have been normalized by $\rho_0 c_0$.

Grazing Incidence Tests

The NASA Langley flow impedance tube (Fig. 2) provides a controlled aeroacoustic environment for measuring acoustic properties of liner specimens in the presence of shearing flow and/or grazing incidence sound. As illustrated in the figure, acoustic drivers generate sound in a 5.08-cm-diam cylindrical tube. The sound is allowed to propagate through an air supply plenum chamber (not used in the present experiment) and transitions into a 5.08 cm^2 test duct which will support only plane wave propagation up to a frequency of about 3.5 kHz. The test section can accommodate a 5.08-cm wide specimen with lengths up to 40.64 cm. A traversing mechanism allows flush mounted microphones to be positioned over a 101.6-cm length starting 76.2 cm upstream of the specimen's leading edge and going about 5.08 cm beyond the trailing edge.

Two types of tests were conducted on the 5.08×40.64 cm liner specimen. In the first test, liner linearity with respect to sound pressure level (SPL) was verified. This was accomplished by placing the control microphone in the plane of the leading edge of the liner test specimen. A second measuring microphone was located just beyond the trailing edge to measure the transmitted SPL. The SPL was then held constant at the control microphone (leading edge) at levels of 110 to 130 dB, while a sine wave sweep was conducted from 0.3-3.4 kHz. In the second test, a single microphone was traversed at constant speed over the entire length of the test section. In this way the details of the wave structure were obtained. A typical grazing incidence standing wave is sketched in Fig. 3. In effect, a right moving plane wave senses an axial impedance change in the vicinity of the liner specimen leading edge and a standing wave is produced. Downstream of the leading edge a decay of the SPL, due to liner absorption, is observed. This is followed by a constant pressure level beyond the trailing edge of the specimen due to the anechoic termination. Upstream of the leading edge, SWRs and ZNULLs are well defined, which implies a well-defined equivalent axial impedance ζ_A at the specimen's leading edge.

For locally reacting liners, it is customary to assume that the normal impedance sensed by a grazing incidence wave to be identical to that sensed by a wave at normal incidence. Measured and calculated wave structures will be compared subsequently in order to check the validity of this assumption for the liner specimens used in the present study.

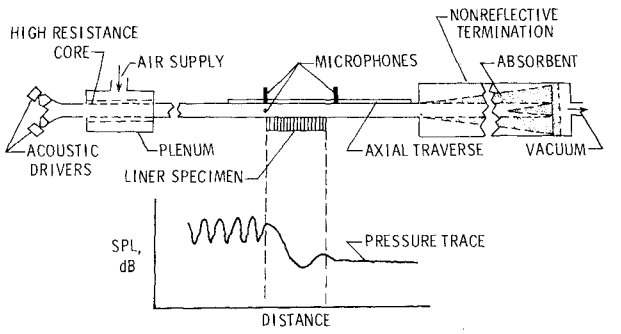

Fig. 2 Flow impedance tube configuration.

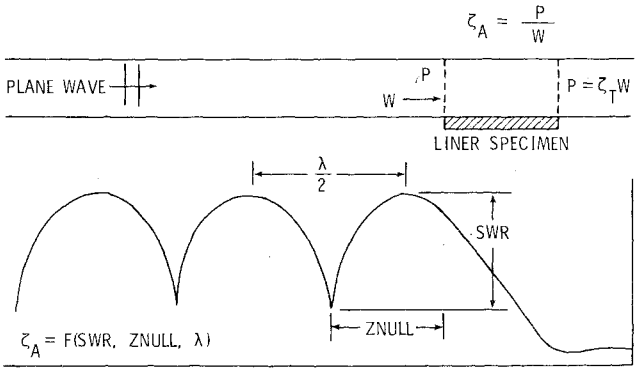

Fig. 3 Typical standing wave—grazing incidence.

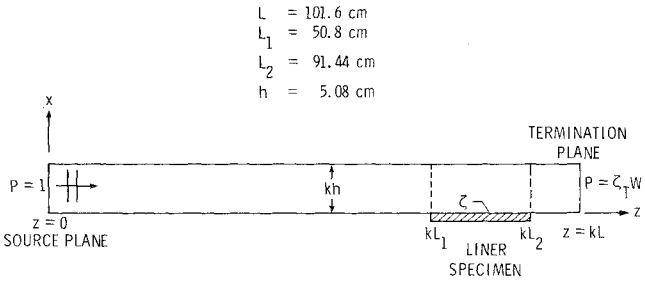

Fig. 4 Impedance tube math model—grazing incidence.

Analysis

The geometrical details for the grazing incidence configuration are shown in Fig. 4. For calculation purposes, the overall length of the impedance tube model was set at $L = 101.6$ cm. This allows slightly more than one wavelength in the upstream hardwall section ($0 \le z \le kL_1$) for the lowest frequency case of 0.3 kHz. The length of the liner specimen was 40.64 cm and the other lengths of interest are indicated in the figure. The tube geometry assures that only the plane wave mode will propagate in the frequency range (0.3-1.2 kHz) considered in this paper. Hence, a uniform pressure condition is assumed at the source plane.

Acoustic Equations

The acoustic pressure in the impedance tube is given by the solution to Helmholtz equation

$$\frac{\partial^2 p}{\partial z^2} + \frac{\partial^2 p}{\partial x^2} + p = 0 \tag{1}$$

and the acoustic particle velocities are found from the momentum equations:

$$u = -j\frac{\partial p}{\partial x} \tag{2}$$

$$w = -j\frac{\partial p}{\partial z} \tag{3}$$

Equations (1-3) are based on an $e^{-j\omega t}$ harmonic time dependence and are expressed in terms of nondimensional variables: acoustic pressure has been normalized by $\rho_0 c_0^2$, the acoustic particle velocity by c_0, and all lengths have been normalized by multiplying by the wavenumber k.

A numerical solution of these equations was achieved by a Galerkin/weighted-residual finite-element algorithm. Details of the procedure are reported in Ref. 5; however, a cubic rectangular element based on Hermite polynomials was employed in this paper.[6,7]

Boundary Conditions

The following boundary conditions were imposed on the finite-element solution (grazing incidence):

Source plane:

$$p(x,0) = 1.0 \tag{4}$$

Termination plane:

$$p(x,kL) = \zeta_T w(x,kL)$$

$$\zeta_T = 1.0 \tag{5}$$

Lower wall:

$$u(0,z) - \frac{p(0,z)}{\zeta(z)} = 0 \tag{6a}$$

$$\frac{1}{\zeta(z)} = \begin{cases} 1/\xi & kL_1 \le z \le kL_2 \\ 0 & \text{elsewhere} \end{cases} \tag{6b}$$

Upper wall:

$$u(kh,z) = 0 \tag{7}$$

Convergence Calculations

Adequate resolution of the standing wave, standing wave ratio (SWR), and null position(ZNULL) were determined by using up to 400 axial and 10 lateral elements. Acceptable convergence was achieved with 200 axial elements and 4 lateral elements, and all finite-element calculations presented herein are based on this spatial discretization.

Discussion of Results

Normal Incidence Wave Structure

Calculations of SWR and null position were made at a number of discrete frequencies using the measured normal incidence impedance values given in Table 1. The purpose of these calculations was to compare measured and predicted wave structures for the simplest experimental configuration possible: a one-dimensional wave field and a locally reacting liner specimen. Results are given in Table 2 and the agreement is excellent over the given frequency range. The SWR values agree to the first decimal place, except at 0.64 kHz where the calculated SWR is high by 0.2 dB. The ZNULL values are in agreement to within 0.06 cm.

Grazing Incidence Wave Structure

Comparison with Experiment

Results from the grazing incidence tests are presented in Table 3 and plotted in Fig. 5. The solid symbols in the figure indicate the calculated (finite element) wave structure. These calculations were based on the measured normal incidence impedance values (Table 1).

A comparison between the measured and calculated wave structure is given in Table 4. Here the measured SWR and ZNULL values are tabulated, along with the corresponding values calculated by the finite-element method. Sound pressure level (SPL) losses over the 40.64-cm length of liner specimen are also listed. The measured and calculated SWR values differ by about 16-63%. The null positions (ZNULL) are in better agreement, but differ by as much as about 21% (0.64 kHz). The calculated SWR, ZNULL, and SPL loss values are derived from centerline pressure values. There were only small variations of these parameters across the width of the impedance tube.

Computational Checks

In view of the differences between the measured and calculated wave structure data for the grazing incidence case, a number of additional calculations were performed to double check the validity of the finite-element math model. The first set of check calculations was done using a Wiener Hopf algorithm developed by Koch in Ref. 8. These data are parenthetically indicated in Table 4 and the comparison with the calculated finite-element data is quite good. For example, the SWR values agree to within 0.1 dB, except at 1.1 kHz where a difference of 0.5 dB is noted. The null positions agree to within 0.5 cm.

A wave propagation math model,[9] which assumes a semi-infinite liner, was also used to check the finite-element calculations. In this math model liner, impedance is a function of the spatial attenuation and phase change in the lined

Table 2 Normal incidence wave structure

	Measured		Calculated	
Frequency, kHz	SWR, dB	ZNULL, cm	SWR, dB	ZNULL, cm
0.30	14.4	54.58	14.4	54.64
0.40	17.7	34.32	17.7	34.36
0.50	19.4	23.28	19.4	23.31
0.64	20.6	13.62	20.8	13.64
0.66	20.2	12.47	20.2	12.47
0.80	11.2	5.49	11.2	5.50
0.90	11.1	1.66	11.1	1.66
1.00	14.1	14.94	14.1	14.96
1.10	15.5	11.20	15.5	11.20

Table 3 Grazing incidence wave structure

Frequency, kHz	ZNULL/λ	ZNULL, cm	SWR, dB	Resistance, θ_A	Reactance, χ_A
0.30	0.453	52.05	16.8	0.158	-0.297
0.32	0.444	47.83	17.7	0.148	-0.360
0.34	0.434	44.00	17.8	0.153	-0.432
0.36	0.423	40.50	17.7	0.166	-0.514
0.38	0.415	37.65	17.8	0.173	-0.578
0.40	0.401	34.56	18.5	0.179	-0.701
0.42	0.387	31.76	18.0	0.216	-0.836
0.44	0.375	29.38	17.2	0.271	-0.962
0.46	0.356	26.68	15.3	0.429	-1.178
0.48	0.339	24.34	12.5	0.738	-1.320
0.50	0.310	21.37	9.5	1.441	-1.307
0.52	0.292	19.36	6.7	1.729	-0.741
0.53	0.285	18.54	4.0	1.478	-0.301
0.54	0.288	18.38	3.5	1.400	-0.266
0.56	0.293	18.04	2.5	1.263	-0.190
0.58	0.295	17.53	1.4	1.141	-0.099
0.60	0.335	19.25	0.7	1.037	-0.073
0.61	0.394	22.26	0.3	0.991	-0.033
0.62	0.475	26.41	0.7	0.926	-0.023
0.64	0.468	25.21	1.8	0.824	-0.067
0.66	0.455	23.76	3.0	0.737	-0.139
0.68	0.433	21.95	3.6	0.729	-0.232
0.70	0.413	20.34	3.3	0.799	-0.276
0.72	0.395	18.91	2.6	0.892	-0.263
0.74	0.394	18.35	1.2	0.959	-0.129
0.75	0.487	22.38	1.6	0.833	-0.025
0.76	0.507	23.00	2.2	0.777	+0.018
0.78	0.495	21.88	4.3	0.610	-0.019
0.80	0.471	20.29	5.8	0.526	-0.135
0.82	0.455	19.13	6.1	0.526	-0.214
0.84	0.455	18.67	6.5	0.504	-0.221
0.86	0.446	17.88	8.6	0.411	-0.299
0.88	0.432	16.92	10.0	0.374	-0.402
0.90	0.415	15.89	10.2	0.404	-0.518
0.92	0.402	15.06	11.0	0.407	-0.627
0.94	0.385	14.12	11.8	0.434	-0.783
0.96	0.366	13.14	12.3	0.510	-0.982
0.98	0.347	12.21	11.8	0.689	-1.176
1.00	0.325	11.20	10.6	1.074	-1.342
1.02	0.302	10.21	8.5	1.633	-1.137
1.04	0.294	9.74	5.4	1.574	-0.546
1.06	0.296	9.63	4.3	1.441	-0.407
1.08	0.289	9.22	3.9	1.444	-0.315
1.10	0.279	8.74	3.1	1.382	-0.179
1.12	0.291	8.96	2.6	1.280	-0.192
1.14	0.290	8.77	2.6	1.284	-0.188

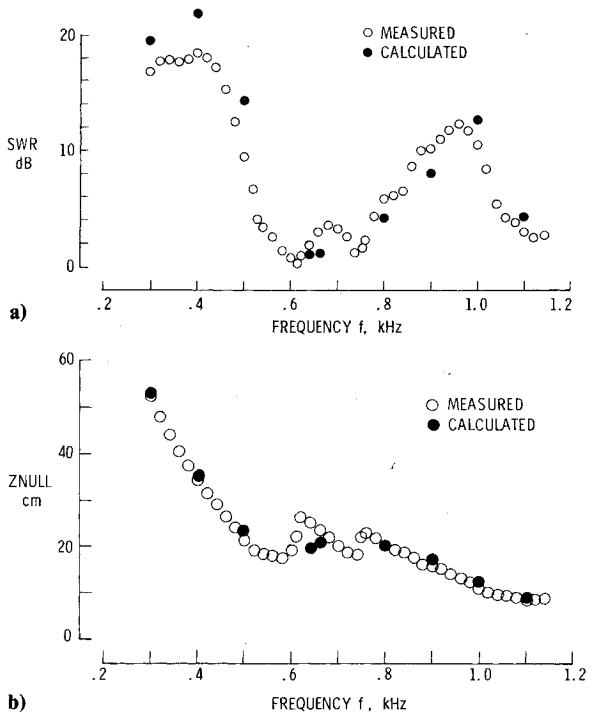

Fig. 5 Measured and calculated wave structure—grazing incidence.

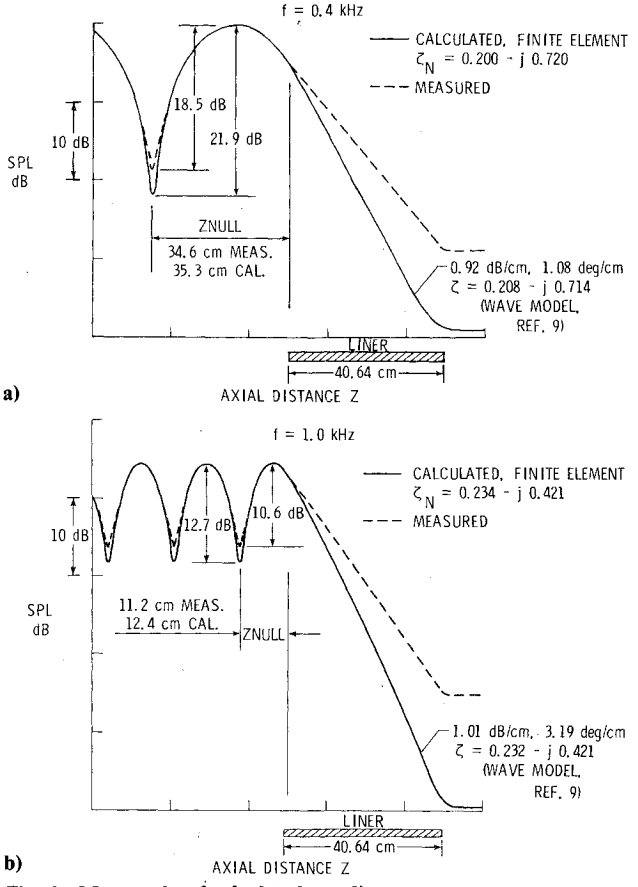

Fig. 6 Measured and calculated standing waves—grazing incidence.

section. In a practical sense, this requires that the liner specimen rapidly attenuate the trailing edge reflection. The waveforms for 0.4 and 1.0 kHz, illustrated in Fig. 6, display these characteristics.

Consider the 0.4 kHz case shown in the first part of Fig. 6. Using the normal incidence impedance value $\zeta_N = 0.200\text{-}j0.720$, the finite-element algorithm returned a calculated value of 21.9 dB for SWR and a null position of 35.3 cm. The measured values (Table 4) are 18.5 dB and 34.6 cm, respectively. The calculated SPL loss of 33.7 dB is 10.3 dB higher than the measured value (23.4 dB)—a considerable difference. From the calculated pressure profile, the spatial attenuation rate (0.92 dB/cm) and rate of change of phase angle (1.08 deg/cm) were determined. Using these data, the wave propagation model returned a grazing incidence impedance value of $\zeta = 0.208\text{-}j0.714$, almost identical to the normal incidence value of $\zeta_N = 0.200\text{-}j0.720$ used in the finite-element calculation. The calculation was repeated for 1.0 kHz (second part of Fig. 6) and the results agree even better. These computational checks (convergence, normal incidence, Wiener Hopf, and wave propagation theory) validate the accuracy of the finite-element model for the purpose of this investigation.

Clearly the calculated grazing incidence wave structure (based on measured normal incidence impedance) differs substantially from the measured wave structure. This discrepancy suggests that the normal impedance presented to the wave field in a grazing incidence configuration differs

Table 4 Grazing incidence wave structure

Frequency, kHz	Measured SWR, dB	Measured ZNULL, cm	Measured SPL loss, dB	Calculated SWR, dB	Calculated ZNULL, cm	Calculated SPL loss, dB
0.3	16.8	52.05	24.5	19.5	52.72	55.0
				(19.5)[a]	(52.36)	(52.8)
0.4	18.5	34.56	23.4	21.9	35.25	33.7
				(21.8)	(35.04)	(32.3)
0.5	9.5	21.37	11.9	14.3	23.14	18.1
				(14.3)	(22.83)	(17.5)
0.64	1.8	25.21	2.0	1.0	19.78	3.4
				(1.0)	(20.08)	(3.2)
0.66	3.0	23.76	1.8	1.1	21.30	3.1
				(1.2)	(21.65)	(3.0)
0.8	5.8	20.29	2.8	4.2	20.20	15.3
				(4.2)	(19.69)	(15.0)
0.9	10.2	15.89	39.0	8.1	17.27	79.5
				(8.1)	(16.93)	(79.0)
1.0	10.6	11.20	28.0	12.7	12.43	41.9
				(12.8)	(12.21)	(40.2)
1.1	3.1	8.74	8.5	4.3	8.99	11.3
				(4.8)	(8.66)	(11.0)

[a] ( ) computed by Wiener-Hopf method (Ref. 8).

from the impedance presented to the wave field in a normal incidence configuration. This angle of incidence effect indicates that the "locally reacting" test liner may be contaminated by "extended reaction" effects. The existence of such effects would not be detected by the normal incidence impedance measurements. Therefore, the two test configurations, used in conjunction with each other, can serve as a means of verifying the existence of extended reaction effects. For the particular test liner used in this investigation, the honeycomb cavities at the edges of the specimen were unavoidably cut by the sawing operation required to remove the test sample from the parent material. It is possible that this produced an extended reaction effect. Further research is needed to verify this hypothesis.

Concluding Remarks

For the nominal locally reacting liner specimen studied in this paper, a finite-element algorithm has been demonstrated to be an accurate analysis tool for correlating normal and grazing incidence acoustic behavior. Differences between measured and predicted standing wave ratio and null position data suggest the presence of extended reaction effects. These effects are most likely due to wave coupling in the edge cavities, although additional research is needed to validate this hypothesis.

Acknowledgments

The authors are indebted to W. Koch for his calculations pertinent to this paper.

References

[1] Zorumski, W. E. and Tester, B. J., "Prediction of the Acoustic Impedance of Duct Liners," NASA TM X 73951, Sept. 1976.

[2] Nayfeh, A. H., Kaiser, J. E., and Telionis, D. P., "Acoustics of Aircraft Engine—Duct Systems," *AIAA Journal*, Vol. 13, Feb. 1975, pp. 130-153.

[3] Beranek, L. L., *Acoustic Measurements*, John Wiley and Sons, Inc., New York, 1949.

[4] Parrott, T. L. and Smith, C. D., "Random and Systematic Measurement Errors in Acoustic Impedance as Determined by the Transmission Line Method," NASA TN D-8520, Dec. 1977.

[5] Abrahamson, A. L., "A Finite Element Algorithm for Sound Propagation in Axisymmetric Ducts Containing Compressible Mean Flow," NASA CR-145209, June 1977.

[6] Lester, H. C. and Parrott, T. L., "Application of Finite Element Methodology for Computing Grazing Incidence Wave Structure in an Impedance Tube: Comparison with Experiment," AIAA Paper 79-0664, March 1979.

[7] Desai, C. S. and Abel, J. F., *Introduction to the Finite Element Method—A Numerical Method for Engineering Analysis*, Van Nostrand Reinhold Publishing Co., 1972.

[8] Koch, W., "Attenuation of Sound in Multi-Element Acoustically Lined Rectangular Ducts in the Absence of Mean Flow," *Journal of Sound and Vibration*, Vol. 52, 1977, pp. 459-496.

[9] Armstrong, D. L., Beckemeyer, R. J., and Olsen, R. F., "Impedance Measurements of Acoustic Duct Liners with Grazing Flow," 87th Meeting of the Acoustical Society of America, April 1974.